3 Biotech (2020) 10:270
https://doi.org/10.1007/s13205-020-02261-x

ORIGINAL ARTICLE

MicroRNA-155 complementation on a chemically functionalized dual electrode surface for determining breast cancer

Subash C. B. Gopinath[1,2] · Veeradasan Perumal[3] · Shijin Xuan[4]

Received: 6 March 2020 / Accepted: 14 May 2020

Abstract

This study correlated and quantified the expression of microRNA-155 with breast cancer to determine breast cancer progression. The target microRNA-155 sequence was identified by complementation on a capture-probe sequence-immobilized interdigitated dual electrode surface. The sensitivity was found to be 1 fM, and the limit of detection fell between 1 and 10 fM. The specific sequence selectivity with single mismatches, triple mismatches, and noncomplementary bases failed to complement the capture-probe sequence. The obtained results demonstrate the selective determination of the microRNA-155 sequence and can help to diagnose breast cancer.

Keywords Breast cancer · microRNA-155 · Interdigitated electrode · Surface chemistry · Biosensor

Introduction

Breast cancer is one of the most common cancers, resulting in unlimited cell proliferation in breast tissue, and is the leading cause of death every year, with >5,000,000 cases worldwide (Zheng et al. 2018). After skin cancer, breast cancer was found to be the most common cancer among women in the United States. The evidence for neoplasias in the past decade showed an increasing trend of breast cancer cases, starting at 9.69 and reaching 14.97 per 100,000 young women during the years

l rates of breast cancer patients are similar when considering patients at the same stage of cancer progression. Usually, 90% of breast cancer patients live for 5 years; however, this percentage and survival period can be improved by proper diagnosis. The mortality rate of breast cancer is increasing due to the lack of detection at earlier stages, which leads to less effective chemotherapy (Huerta-Nuñez et al. 2019). Ultrasound scanning, X-ray mammography, and magnetic resonance imaging are generally used to diagnose breast cancer (Brooks et al. 2009; Dromain et al. 2013; Rodríguez-Ruiz et al. 2019). However, these techniques often have lower sensitivity, poor cost-effectiveness, and difficulty diagnosing at earlier stages (Selwyna et al. 2013). In particular, the common mammography technique is not suitable for women with dense breasts (Brooks et al. 2009). Thus, it is mandatory to develop a sensitive and user-friendly biomolecular diagnostic method for breast cancer with a suitable biomarker (Chang et al. 2014; Cui et al. 2017; Sountharrajan et al. 2017).

Various blood-based biomarkers, such as estrogen receptor (ER), the hormone receptor HER2, progesterone receptors, BRCA1 protein, and circulating tumor DNA, have been shown by researchers to facilitate breast cancer diagnosis (James et al. 2007; Zhang et al. 2011; Duffy et al. 2017, 2018; Salahandish et al. 2018). Among such biomarkers, microRNA-based detection has received

✉ Shijin Xuan
xyshijina@sina.com

Subash C. B. Gopinath
subash@unimap.edu.my

Veeradasan Perumal
veeradasan.perumal@utp.edu.my

1 School of Bioprocess Engineering, Universiti Malaysia Perlis, 02600 Arau, Perlis, Malaysia

2 Institute of Nano Electronic Engineering, Universiti Malaysia Perlis, 01000 Kangar, Perlis, Malaysia

3 Mechanical Engineering Department, Universiti Teknologi PETRONAS, 32610 Seri Iskandar, Perak Darul Ridzuan, Malaysia

4 Department of Mammary and Thyroid Surgery, Central Hospital Affiliated to Shandong First Medical University, No. 105 Jiefang Road, Lixia District, 250013 Jinan, Shandong Province, People's Republic of China

Published online: 28 May 2020

great attraction from researchers due to its high sensitivity and selective detection for various diseases including breast cancer (Svoboda et al. 2012; Wang and Luo 2015). MicroRNA is a single-stranded RNA that functions as a negative regulator of posttranscriptional modification in most biological processes. MicroRNA expression under abnormal conditions is highly correlated with different types of cancers including breast cancer (Cardoso et al. 2016; Zhang et al. 2018). In particular, studies on tumor suppression microRNA and oncogenic microRNA have been more focused for diagnostic purposes. More specifically, microRNA-155 is abnormally expressed in patients with breast cancer (Jiang et al. 2010; Mattiske et al. 2012). Based on an earlier study by Zheng et al. (2012), the relative median expression of miR-155 ($2-\Delta\Delta Ct$) was 0.360 in breast tumor samples, and the nontumor control had a value of 0.135, showing threefold differences in miRNA-155 expression between normal and tumor cells. On the other hand, recently, Zhang et al. (2019) revealed that miR-155-3p was upregulated in breast cancer cells but normally expressed in breast MCF 10A cells. However, the mRNA and protein levels of cell adhesion molecule 1 displayed a different pattern with opposite expression, as miR-155-3p negatively regulated cell adhesion molecule 1 expression (in MCF-7 breast cancer cells). In addition, miR-155-3p expression enhanced tumorigenesis and cell proliferation and repressed cell apoptosis. Therefore, developing a simple and rapid diagnostic method for microRNA-155 is beneficial for identifying breast cancer at its initial stage. In this research, the target microRNA-155 was detected by a suitable capture probe on an interdigitated electrode (IDE) sensing surface.

Special attention has been paid to breast cancer research by incorporating a nanotechnological approach, especially with biodegradable polymeric nanoparticles, which has led to several improvements, as stated by Ahmad and colleagues. The biodegradable polymeric nanoparticles acts as drug carriers, as suggested by in vitro and in vivo studies (Alam et al. 2016; Ahmad et al. 2018a,b, 2019). In the current research, different nanotechnological approaches have been used for in vitro analysis with a nanoscale IDE, which was fabricated and efficiently used to detect the target microRNA-155. The capture probe was immobilized on the IDE surface by using a biotin–streptavidin complex, and the target microRNA-155 was determined (Lv et al. 2019). IDE sensors have been well established with transducers and are widely accepted in various applications including chemical and biological sensors. Due to the relatively easy fabrication steps, high sensitivity, ease of use, and low cost, IDEs are attractive in the field of biosensors and can be potentially used to identify biological ligands such as RNA, DNA, aptamers, antibodies, and proteins (Cheen et al. 2017; Letchumanan et al. 2019a,b; Ramanathan et al. 2019). A unique probe, microRNA, was used in the present investigation to make further progress in the diagnosis of breast cancer biomarkers.

Materials and methods

Reagents and biomolecules

Phosphate-buffered saline (PBS), streptavidin, and (3-glycidyloxypropyl)trimethoxy silane (GOPTS) were purchased from Sigma-Aldrich (USA). Ethanolamine was purchased from Fisher Scientific, UK. Biotinylated capture probes and targets were synthesized commercially and received from the local supplier as follows: 5′-ACCCCUAUCACGAUUAGCAUUAA-A_{24}-3′ [capture-probe]; 5′-UUAAUGCUAAUCGUGAUAGGGGU-3′ [target]; 5′-AAUUACGAUUAGCACUAUCCCCA-3′ [noncomplementary]; 5′-UUAAUGCUAAACGUGAUAGGGGU-3′ [single-mismatch]; 5′-UUAAUGCUUUACGUGAUAGGGGU-3′ [triple-mismatch]; and 5′-biotinylated-dT_{20} (for surface immobilization). All these oligos were designed based on previous research (Hakimian et al. 2018).

Pattern design on a chrome mask

Initially, the pattern of the dielectric sensor was designed using AutoCAD software. The pattern was printed on a blank photomask and pasted on the surface of chrome glass. This chrome glass was fixed under a UV exposure system for the pattern transferring procedure. A silicon dioxide substrate with an aluminum thin film deposited on it was placed in the opposite direction against the chrome glass and exposed to UV light for 10 s. The pattern was transferred followed by a developing process using the resist developer.

Fabrication of the interdigitated electrode (IDE)

The surface electrode was produced via a conventional microelectronic fabrication process with the following steps (Letchumanan et al. 2019b): (i) A 4-in. wafer with existing native oxide was prepared; (ii) the wafer was cleaned using buffered oxide etch (BOE) and piranha solution to remove the native oxide and inorganic contaminants; (iii) a 2800 Å-thick oxide layer was grown on the surface via an hour of wet thermal oxidation at 1000°C; (iv) the oxide layer-coated wafer was cut into four pieces for better handling; (v) a metal layer of aluminum was deposited as an adhesion layer for the conductive layer, and the aluminum layer (40 nm), which was produced via a thermal evaporator-based physical deposition method, was 3 cm long and 0.5 mm in diameter; (vi) a layer of positive photoresist was spin-coated on the substrate; (vii) the wafer was soft-baked at 90°C for 60 s; (viii) the wafer was aligned with a chrome

mask and exposed to UV light for 10 s; (ix) the wafer was rinsed in RD6 developer solution within 15 s to remove the unexposed area, resulting in an oxide IDE pattern; (x) the wafer was hard-baked at 90°C for 120 s; (xi) the wafer was etched using aqua regia to remove the exposed area of both layers and finally, (xii) the surface pattern was produced, and the remaining photoresist was washed away using acetone. 3D nanoprofilometry (Hawk 3D-profilometry, USA) analysis was carried out to observe the clear-cut image of gaps between the electrodes. Current measurements (A) were performed using a Keithley 6487 picoammeter with a linear sweep of 0–2 V at a step of 0.1 V (at 20 s).

Capture-probe immobilization on the IDE sensor

The capture probe was immobilized on the IDE surface by biotin–streptavidin complex formation. Initially, the IDE sensing surface was modified with GOPTS by adding a diluted GOPTS solution dropwise and incubating for 1 h. After incubation, the surface was washed with PBS buffer to remove the unbound free GOPTS. Then, 200 nM streptavidin was added to the GOPTS-modified surface for 1 h, and the surface was subsequently blocked by 1 M ethanolamine for 30 min at room temperature. Next, 1 µM biotinylated capture probe was added to the surface and incubated for 10 min at room temperature. The capture-probe-immobilized IDE was utilized to quantify the target microRNA-155.

Detection of microRNA-155 complementation on the capture-probe-immobilized IDE surface

The capture-probe-modified IDE was utilized to determine the complementation of target microRNA-155. The current was noted at this point. Then, the target at 10 pM was added to the surface and allowed to stand for 15 min for complementation on the capture probe. After washing the surface, the current was noted again, and the changes in current before and after target complementation were considered as representing the real interaction for the complementation between the target and capture probe.

Limit of detection on complementation by microRNA-155

To estimate the detection limit with microRNA-155, target concentrations from 1 fM to 10 pM were prepared by tenfold dilutions and added (as 10 µl aliquots) to the capture-probe-modified IDE surface. After 10 min of reaction, the surface was washed thoroughly with PBS to remove the unbound molecules. The changes in current before and after addition of the target were noted for comparison. The difference in current was calculated and plotted by Excel software to obtain the limit of detection by linear regression.

Control experiments for microRNA-155 target complementation

Control experiments were carried out to evaluate the specific detection of the target molecule, microRNA-155. The single-mismatch, triple-mismatch, and complementary oligonucleotides of target sequences at a concentration of 10 fM were independently added on the capture-probe-modified IDE surfaces, and the changes in current were compared with the current observed for the specific complementation of the target sequence.

Results and discussion

In this research, the breast cancer biomarker microRNA-155 was detected by an immobilized capture probe on an interdigitated electrode (IDE) sensor. Figure 1 depicts the schematic representation of microRNA-155 detection on the IDE sensor. The fabricated surface was observed via 3D nanoprofilometry, and the observed image clearly showed the presence of gap and finger regions along the electrode (Fig. 2a). The image reflects the original dimensions of the IDE: 7500 µm length; 4100 µm width; 20 finger-gap pairs; 85 µm gap size; 100 µm electrode size; 40 nm electrode thickness; and 4000 µm finger length. The IDE comprises a silica surface on which an aluminum electrode was deposited. This setup operates based on the dipole moment on the surface; upon binding of molecules, there will be variation in the dipole moment with the concomitant alternation in the current (Fig. 2a, inset). The capture probe was immobilized on IDE through the biotin–streptavidin strategy. A 5′-biotinylated polyT (biotin-dT_{20}) oligo was synthesized separately and duplexed with the capture probe extended by polyA (A_{24}) [5′-ACCCCUAUCACGAUUAGCAUUAA-A_{24}-3′]. A four-base spacer was created between this complementation and the sequences of the capture probe to create flexibility. This complex was attached to a streptavidin-immobilized IDE sensing surface through the chemical linker GOPTS. This tetravalent binding strategy helps increase the number of capture probes on the sensing surface (Duan et al. 2012). Amine groups on streptavidin can interact with epoxy molecules originating from GOPTS. The target microRNA-155 was complemented with the complexed capture probe on the modified IDE surface.

Capture-probe immobilization on the IDE through a biotin–streptavidin strategy

Figure 2b shows the current change from each modification step while immobilizing the capture probe. The current of the GOPTS-modified IDE surface was noted as 5.70E−08 A, and after the surface modification with streptavidin, the

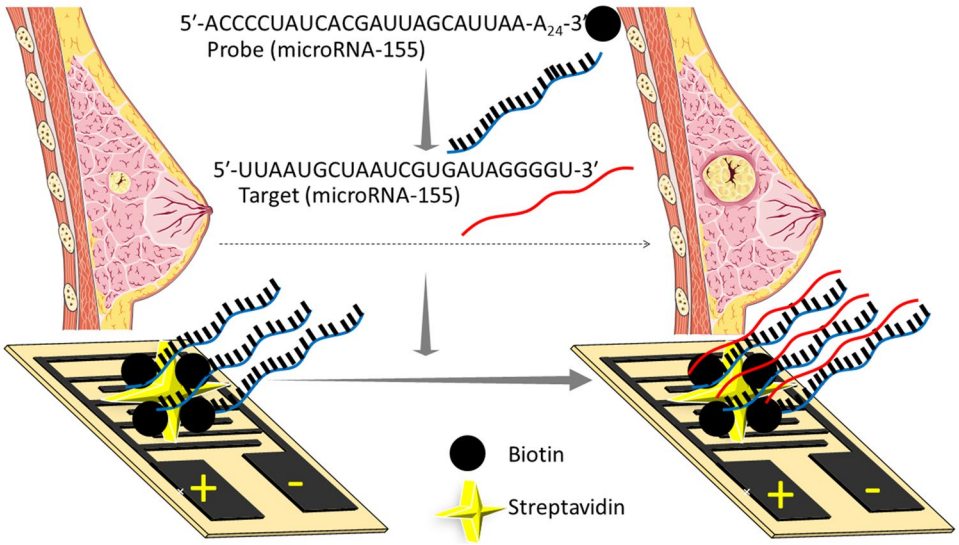

Fig. 1 Schematic representation of the detection strategy. Capture DNA was attached to an IDE through a biotin–streptavidin strategy. Streptavidin was immobilized through a GOPTS chemical linker. Then, a biotinylated capture probe was added and complemented by the target microRNA-155

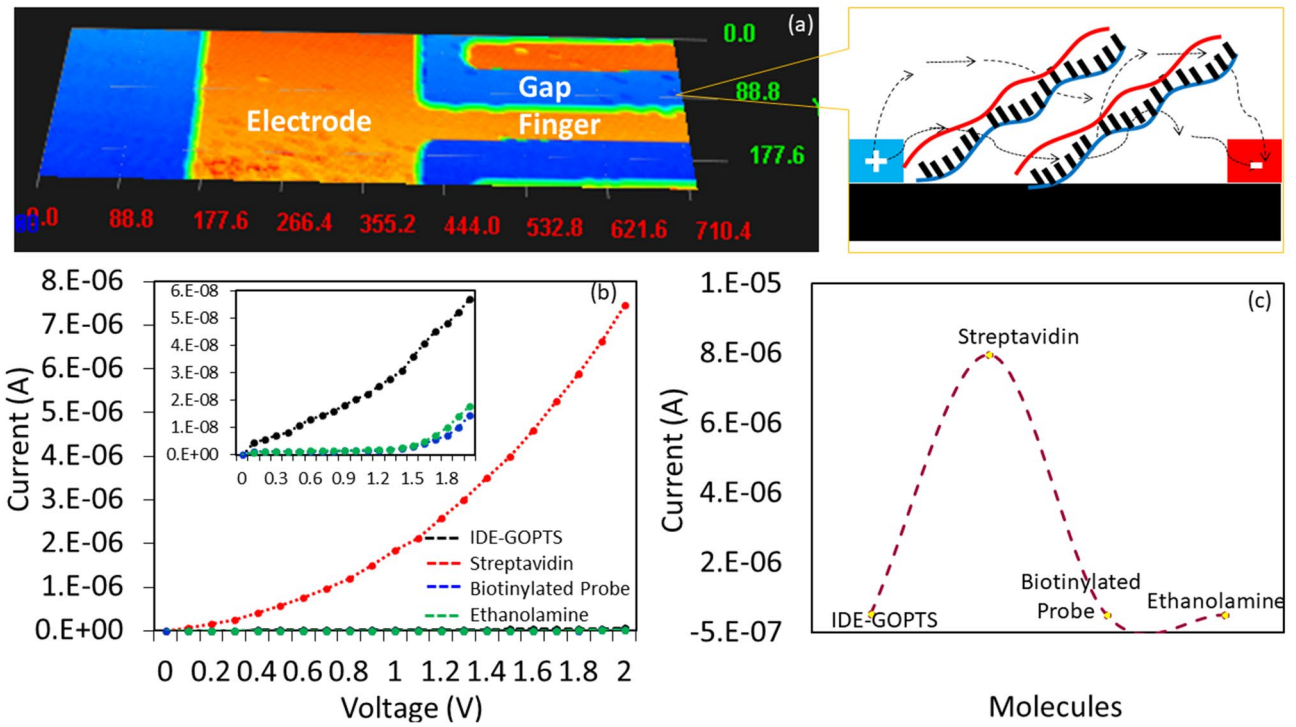

Fig. 2 **a** Surface profile of the IDE under 3D profilometry. Gap, finger and electrode regions are shown. A mechanism of the dipole moment is shown. **b** Capture-probe immobilization on the IDE sensor. Clear current changes were noted after each immobilization process, indicating the successful attachment of the capture probe on the IDE surface. The enlarged portion is shown as the figure *inset*. **c** Changes in current for each immobilization step. Ethanolamine shows a smaller current change due to less space availability on the GOPTS surface

value increased to 7.47E−06 A. These changes in current confirm streptavidin attachment on the IDE sensing surface. Subsequently, the current of the biotinylated capture probe on the streptavidin-modified surface drastically decreased to 1.44E−08 A. These results show a different trend due to the charge differences of the molecules attached on the surface. These current changes occurred due to the chemical interaction of streptavidin with the GOPTS surface. This process confirms the immobilization of the capture probe on the GOPTS-modified IDE surface (Fig. 2b, c).

Complementation of microRNA-155 on the capture-probe-modified IDE surface

The target microRNA-155 sequence [5′-UUAAUGCUAAUCGUGAUAGGGGU-3′] was detected by complementation on a capture-probe-modified IDE surface. Before detection, to avoid biofouling, after the surface was modified with the capture probe, the excess GOPTS surface was covered with ethanolamine. As shown in Fig. 2c, after adding ethanolamine, the current was increased slightly to 1.79E−09 A. This slight change occurred because the GOPTS surface was nearly completely occupied by streptavidin, so ethanolamine could bind to the small remaining area of the GOPTS-modified surface. After the surface was blocked by ethanolamine, the target at a concenteration of 10 pM was complemented on the surface, and the current was drastically increased to 1.01E−06 A (Fig. 3a). This current change clearly indicates the complemetation of the target with the capture probe immobilized on the IDE surface. The changes in the current direction are based on the charge on the surface of the biomolecule. For example, a single-stranded probe possesses a phosphate backbone with a negative charge and shows a decreasing trend from that of streptavidin. However, when a duplex forms, the above trend is reversed due to the masking effect of the phosphate backbone by the second strand.

Limit of detection for complementing microRNA-155

The limit of detection with microRNA-155 target sequence complementation was estimated by carrying out an experiment with different concentrations of target complemented with the capture probe. The target at concentrations of 100 aM, 1 fM, 10 fM, 100 fM, 1 pM, and 10 pM was dropped individually on the capture-probe-modified surfaces, and then, the changes in current were observed (Fig. 3b). When 100 aM target sequence was added, the current increased from 1.79E−08 to 2.45E−08 A. This increased current indicates the complementation of the target and capture probe. Further, when the target concentration was increased to 1 fM, the current increased to 2.9E−08 A. With 10 fM target sequence, the current was drastically increased to 6.35E−07 A. With further increases in the concentration of the target sequence, the current gradually increased. At concentrations of 100 fM, 1 pM, and 10 pM, the current levels were 6.25, 8.25, and 9.37E−07 A, respectively. As seen until 1 fM, only smaller changes in current were noted; from 10 fM, the current increased drastically, and there was not much difference with the concentrations of 1 pM and 10 pM, indicating a close approach to the saturation point (Fig. 4a). The difference in current was plotted by a linear regression graph, and the limit of detection was calculated (S/N = 3:1; LOD = standard deviation of the baseline + 3σ) in the range between 1 and 10 fM. Further, the sensitivity was found to be 1 fM (Fig. 4b).

Control experiments for specific complementation of microRNA-155

Control experiments were carried out with three different control sequences, namely single-mismatch, triple-mismatch, and complementary target sequences 5′-UUAAUGCUAAACGUGAUAGGGGU-3′ [single-mismatch]; 5′-UUAAUGCUUUACGUGAUAGGGGU-3′

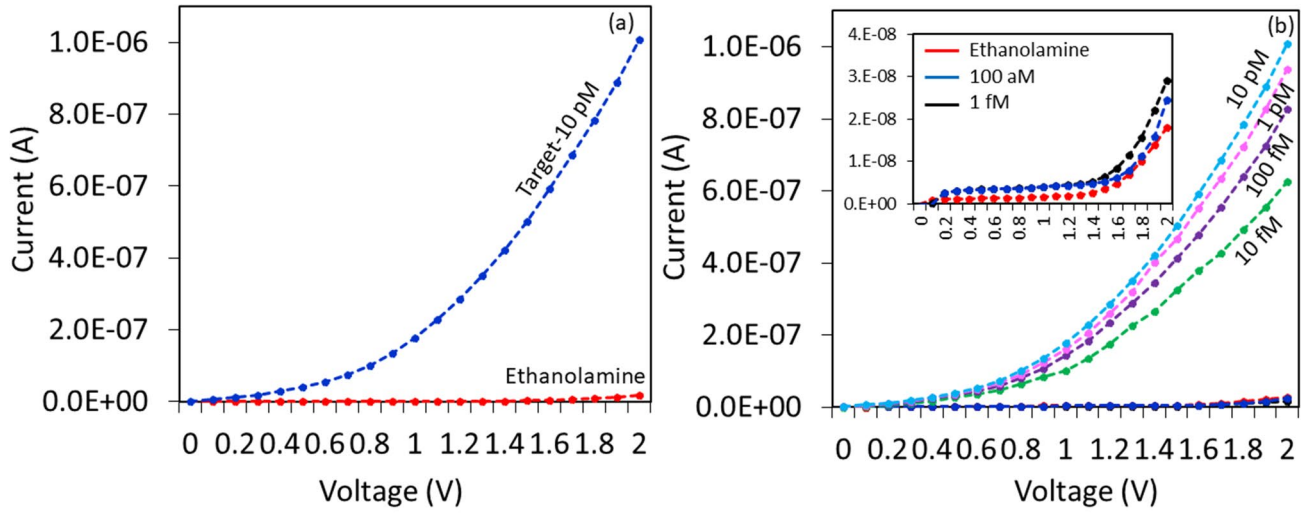

Fig. 3 **a** Target microRNA-155 detection. The current was drastically increased with 10 pM of target and capture complementation. **b** MicroRNA-155 titration on the capture probe. Target concentrations from 100 aM to 10 pM were complemented on the IDE-capture surface, and the current levels were increased depending on the target concentration. The enlarged portion is shown as the figure inset

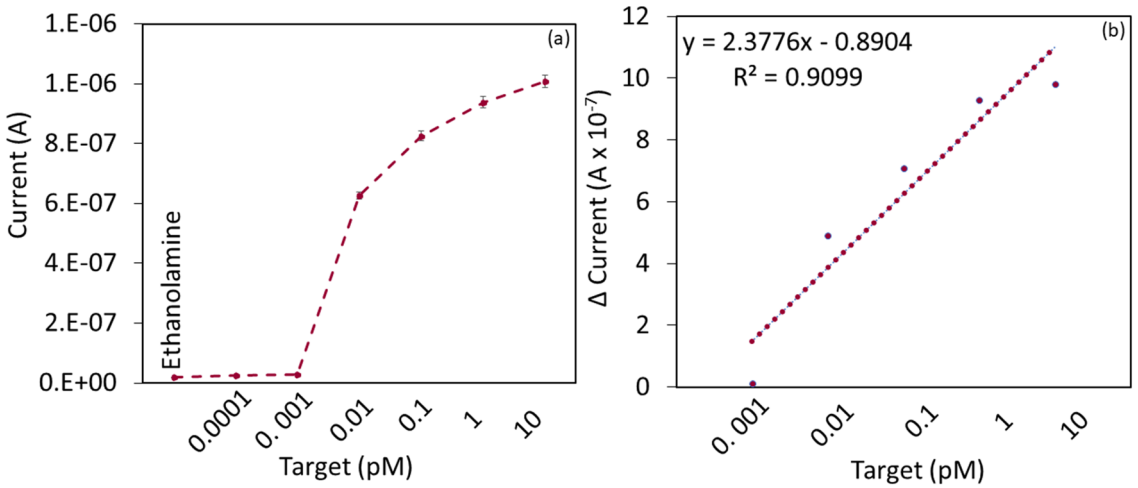

Fig. 4 **a** Graph of the current with the target from 100 aM to 10 pM. With increasing target concentrations, the current gradually increased. From 1 fM, the current increased. **b** Difference in current with target concentrations. Concentrations from 100 aM to 10 pM were plotted in an Excel file, and the limit of target detection was calculated by linear regression analysis

[triple-mismatch]; 5′-AAUUACGAUUAGCACUAU CCCCA-3′ [noncomplementary]. These three sequences at concentrations of 10 fM were complemented independently with the capture probe and compared with target capture-probe complementation. As shown in Fig. 5a, none of these control sequences yielded significant changes in the current, while the target sequence showed a great change in the current. These results supported the conclusion that the IDE system demonstrated in this study specifically detects microRNA-155 with a higher discrimination than that against other molecules. To prove the high performance, the variations among different devices and the obtained average values are displayed in Fig. 5b.

Different sensing strategies have been recently demonstrated for the detection of breast cancer, including optical, electrochemical, and microwave-based detection approaches (Liu et al. 2019; Aldhaeebi et al. 2020; An et al. 2020; Kim et al. 2020; Loyez et al. 2020). Among these sensing strategies, microwave-based detection is totally different from imaging analysis. Other studies mentioned above use unique biomarkers, as in the current study, to reveal the different sensing approaches. The uniqueness is from the detection of exosomal proteins, exosomal miRNAs, and aptamers as probes against cancer cells. Considering these methods by comparison with the current study, there is similarity in terms of the performance, with the differences ranging from

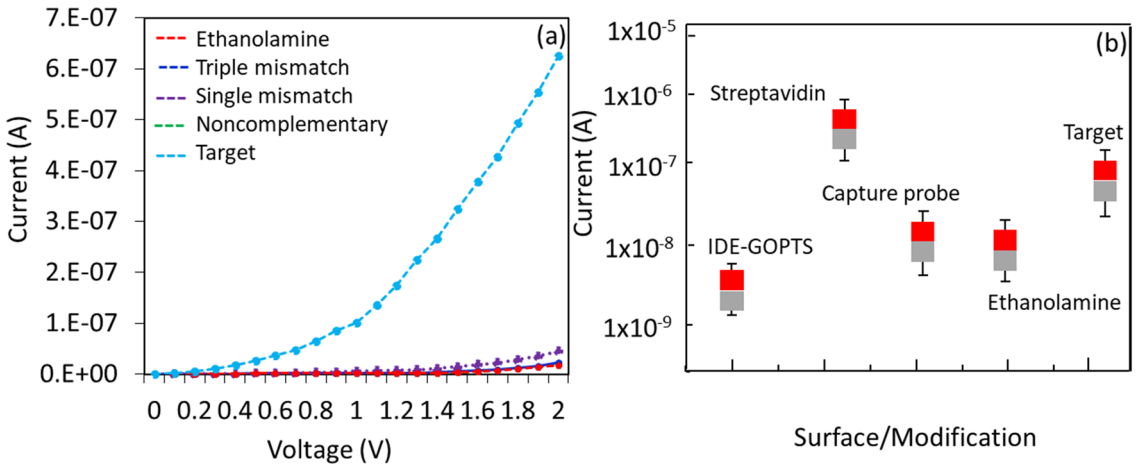

Fig. 5 High-performance analysis. **a** Control experiments for the selective complementation of microRNA-155. Single-mismatch, triple-mismatch and noncomplementary target sequences were complemented on the IDE capture-probe surface, and the current changes were recorded. No significant changes were noted with the control sequences compared to the specific target. **b** Reproducibility on the sensing surface. The averaged data from different devices are shown.

~10- to 100-fold. However, the present study shows other advantages including lower sample consumption, lower operating current, and lower cost. Further, this study uses nanomaterials to compete with current cutting-edge technologies, which are lacking in other previously developed sensors.

Conclusion

Diagnosing breast cancer at the initial stage is mandatory to avoid metastasis of the cancer cells to other tissues. microRNA-155 is a suitable biomarker to diganose breast cancer. The present research focused on identifying the microRNA-155 target sequence by using a capture probe on an interdigitated electrode sensor. The capture probe was linked on the IDE sensor by the chemical linker GOPTS and complemented by the target sequence. It was observed that with increasing target sequence concentrations, the current changes gradually increased. The detection limit was found to be in the range between 1 and 10 fM, with a sensitivity of 1 fM. Moreover, controls with single-mismatch, triple-mismatch and noncomplementary sequences did not significantly increase the current levels, indicating the selective complementation of microRNA-155. This detection strategy helps to diagnose breast cancer and is comparable to currently available sensor approaches, albeit with several advantages.

Author contributions All authors have contributed to the preparation of the manuscript and discussion. All authors read and approved the final manuscript.

Compliance with ethical standards

Conflict of interest All authors have no conflict of interest and agreed with this submission.

References

Ahmad N, Ahmad R, Alam MA et al (2019) Daunorubicin oral bioavailability enhancement by surface coated natural biodegradable macromolecule chitosan based polymeric nanoparticles. Int J Biol Macromol 128:825–838. https://doi.org/10.1016/j.ijbiomac.2019.01.142

Ahmad N, Ahmad R, Alam MA, Ahmad FJ (2018a) Enhancement of oral bioavailability of doxorubicin through surface modified biodegradable polymeric nanoparticles. Chem Cent J 12:65. https://doi.org/10.1186/s13065-018-0434-1

Ahmad N, Alam MA, Ahmad R et al (2018b) Improvement of oral efficacy of Irinotecan through biodegradable polymeric nanoparticles through in vitro and in vivo investigations. J Microencapsul 35:327–343. https://doi.org/10.1080/02652048.2018.1485755

Alam MA, Ahmad N, Ahmad R et al (2016) Quantification of tamoxifen polymeric nanoparticles in female rodent breast tissue by UPLC/ESI-Q-TOF MS/MS. J Young Pharm 8:415–423. https://doi.org/10.5530/jyp.2016.4.18

Aldhaeebi MA, Alzoubi K, Almoneef TS et al (2020) Review of microwaves techniques for breast cancer detection. Sensors (Switzerland) 20:1–38. https://doi.org/10.3390/s20082390

An Y, Li R, Zhang F, He P (2020) An, Y., Li, R., Zhang, F., and He, P. (2020). Magneto-mediated electrochemical sensor for simultaneous analysis of breast cancer exosomal proteins. Anal Chem 92:5404–5410. https://doi.org/10.1021/acs.analchem.0c00106

Brooks AD, Nover AB, Jagtap S et al (2009) Modern breast cancer detection: a technological review. Int J Biomed, Imaging, p 902326

Cardoso AR, Moreira FTC, Fernandes R, Sales MGF (2016) Novel and simple electrochemical biosensor monitoring attomolar levels of miRNA-155 in breast cancer. Biosens Bioelectron 15:621–630. https://doi.org/10.1016/j.bios.2016.02.035

Chang K, Pi Y, Lu W et al (2014) Label-free and high-sensitive detection of human breast cancer cells by aptamer-based leaky surface acoustic wave biosensor array. Biosens Bioelectron 60:318–324. https://doi.org/10.1016/j.bios.2014.04.027

Cheen OC, Gopinath SCB, Perumal V et al (2017) Aptamer-based impedimetric determination of the human blood clotting factor IX in serum using an interdigitated electrode modified with a ZnO nanolayer. Microchim Acta 184:117–125. https://doi.org/10.1007/s00604-016-2001-6

Cui M, Wang Y, Wang H et al (2017) A label-free electrochemical DNA biosensor for breast cancer marker BRCA1 based on self-assembled antifouling peptide monolayer. Sens Actuators B Chem 244:742–749. https://doi.org/10.1016/j.snb.2017.01.060

Dromain C, Boyer B, Ferré R et al (2013) Computed-aided diagnosis (CAD) in the detection of breast cancer. Eur J Radiol 82:417–423. https://doi.org/10.1016/j.ejrad.2012.03.005

Duan X, Li Y, Rajan NK et al (2012) Quantification of the affinities and kinetics of protein interactions using silicon nanowire biosensors. Nat Nanotechnol 7:401–407. https://doi.org/10.1038/nnano.2012.82

Duffy MJ, Harbeck N, Nap M et al (2017) Clinical use of biomarkers in breast cancer: Updated guidelines from the European group on tumor markers (EGTM). Eur J Cancer 75:284–292

Duffy MJ, McDermott EW, Crown J (2018) Blood-based biomarkers in breast cancer: from proteins to circulating tumor cells to circulating tumor DNA. Tumor Biol 40:1–11

Hakimian F, Ghourchian H, Hashemi AS et al (2018) Ultrasensitive optical biosensor for detection of miRNA-155 using positively charged Au nanoparticles. Sci Rep 8:2943. https://doi.org/10.1038/s41598-018-20229-z

Huerta-Nuñez LFE, Gutierrez-Iglesias G, Martinez-Cuazitl A et al (2019) A biosensor capable of identifying low quantities of breast cancer cells by electrical impedance spectroscopy. Sci Rep 9:6419. https://doi.org/10.1038/s41598-019-42776-9

James CR, Quinn JE, Mullan PB et al (2007) BRCA1, a potential predictive biomarker in the treatment of breast cancer. Oncologist 12:142–215. https://doi.org/10.1634/theoncologist.12-2-142

Jiang S, Zhang HW, Lu MH et al (2010) MicroRNA-155 functions as an oncomiR in breast cancer by targeting the suppressor of cytokine signaling 1 gene. Cancer Res 70:3119–3127. https://doi.org/10.1158/0008-5472.CAN-09-4250

Kim S, Kim TG, Lee SH et al (2020) Label-free surface-enhanced raman spectroscopy biosensor for on-site breast cancer detection using human tears. ACS Appl Mater Interface 12:7897–7904. https://doi.org/10.1021/acsami.9b19421

Letchumanan I, Gopinath SCB, Md Arshad MK et al (2019a) Gold nano-urchin integrated label-free amperometric aptasensing human blood clotting factor IX: a prognosticative approach for "royal disease". Biosens Bioelectron 131:128–135. https://doi.org/10.1016/j.bios.2019.02.006

Letchumanan I, Md Arshad MK, Balakrishnan SR, Gopinath SCB (2019b) Gold-nanorod enhances dielectric voltammetry detection of c-reactive protein: a predictive strategy for cardiac failure. Biosens Bioelectron 130:40–47. https://doi.org/10.1016/j.bios.2019.01.042

Liu L, Lu H, Shi R et al (2019) Synergy of peptide-nucleic acid and spherical nucleic acid enabled quantitative and specific detection of tumor exosomal MicroRNA. Anal Chem 91:13198–13205. https://doi.org/10.1021/acs.analchem.9b03622

Loyez M, Hassan EM, Lobry M et al (2020) Rapid detection of circulating breast cancer cells using a multiresonant optical fiber aptasensor with plasmonic amplification. ACS Sens 5:454–463. https://doi.org/10.1021/acssensors.9b02155

Luna-abanto J, Ruiz LG, Laura-martinez J, Tairo-cerron T (2020) Cancer incidence and mortality trends in young adults in Metropolitan Lima young adults, 1990–2012. Cancer Med Sci 14:1–13

Lv Q, Wang Y, Su C et al (2019) Human papilloma virus DNA-biomarker analysis for cervical cancer: signal enhancement by gold nanoparticle-coupled tetravalent streptavidin-biotin strategy. Int J Biol Macromol 134:354–360. https://doi.org/10.1016/j.ijbiomac.2019.05.044

Mattiske S, Suetani RJ, Neilsen PM, Callen DF (2012) The oncogenic role of miR-155 in breast cancer. Cancer Epidemiol Biomark Prev 21(8):1236–1243

Ramanathan S, Gopinath SCB, Md Arshad MK et al (2019) Assorted micro-scale interdigitated aluminium electrode fabrication for insensitive electrolyte evaluation: zeolite nanoparticle-mediated micro- to nano-scaled electrodes. Appl Phys A 125:548. https://doi.org/10.1007/s00339-019-2833-0

Rodríguez-Ruiz A, Krupinski E, Mordang JJ et al (2019) Detection of breast cancer with mammography: effect of an artificial intelligence support system. Radiology 290:1–10. https://doi.org/10.1148/radiol.2018181371

Salahandish R, Ghaffarinejad A, Naghib SM et al (2018) Nano-biosensor for highly sensitive detection of HER2 positive breast cancer. Biosens Bioelectron 117:104–111. https://doi.org/10.1016/j.bios.2018.05.043

Selwyna PGC, Loganathan PR, Begam KH (2013) Development of electrochemical biosensor for breast cancer detection using gold nanoparticle doped CA 15–3 antibody and antigen interaction. In: International conference on signal processing, image processing and pattern recognition 2013, ICSIPR 2013. pp 75–81

Sountharrajan S, Karthiga M, Suganya E, Rajan C (2017) Automatic classification on bio medical prognosis of invasive breast cancer. Asian Pacific J Cancer Prev 18:2541–2544. https://doi.org/10.22034/APJCP.2017.18.9.2541

Svoboda M, Sana J, Redova M et al (2012) MiR-34b is associated with clinical outcome in triple-negative breast cancer patients. Diagn Pathol 7:31

Wang W, Luo Y (2015) MicroRNAs in breast cancer: oncogene and tumor suppressors with clinical potential. J Zhejiang Univ Sci B 16(18):31

Zhang G, Zhong L, Luo H, Wang S (2019) MicroRNA-155-3p promotes breast cancer progression through down-regulating CADM1. Oncol Targets Ther 12:7993–8002. https://doi.org/10.2147/OTT.S206180

Zhang GJ, Huang MJ, Ang JJ et al (2011) Self-assembled monolayer-assisted silicon nanowire biosensor for detection of protein–DNA interactions in nuclear extracts from breast cancer cell. Biosens Bioelectron 26:3233–3239. https://doi.org/10.1016/j.bios.2010.12.032

Zhang J, Wang LL, Hou MF et al (2018) A ratiometric electrochemical biosensor for the exosomal microRNAs detection based on bipedal DNA walkers propelled by locked nucleic acid modified toehold mediate strand displacement reaction. Biosens Bioelectron 102:33–40. https://doi.org/10.1016/j.bios.2017.10.050

Zheng SR, Guo GL, Zhang W et al (2012) Clinical significance of miR-155 expression in breast cancer and effects of miR-155 ASO on cell viability and apoptosis. Oncol Rep 27:1149–1155. https://doi.org/10.3892/or.2012.1634

Zheng Z, Wu L, Li L et al (2018) Simultaneous and highly sensitive detection of multiple breast cancer biomarkers in real samples using a SERS microfluidic chip. Talanta 188:507–515. https://doi.org/10.1016/j.talanta.2018.06.013